Penicillin-binding proteins exhibit catalytic redundancy during asymmetric cell division in *Clostridioides difficile*

Shailab Shrestha[1,2†], Jules M. Dressler[1,2], Morgan E. McNellis[1,2], & Aimee Shen[1,*]

[1]Department of Molecular Biology and Microbiology, Tufts University School of Medicine, Boston, MA, USA.

[2]Program in Molecular Microbiology, Tufts University Graduate School of Biomedical Sciences, Boston, MA, USA.

[†] Current address: Department of Microbiology, Harvard Medical School, Boston, MA, USA.

*Address correspondence to aimee.shen@tufts.edu

Abstract

Peptidoglycan synthesis is an essential driver of bacterial growth and division. The final steps of this crucial process involve the activity of SEDS family glycosyltransferases that polymerize glycan strands and class B penicillin-binding protein (bPBP) transpeptidases that cross-link them. While most bacteria encode multiple bPBPs that perform specialized roles during specific cellular processes, some bPBPs can play redundant roles that are important for resistance against certain cell wall stresses. Our understanding of these compensatory mechanisms, however, remains incomplete. Endospore-forming bacteria typically encode multiple bPBPs that drive morphological changes required for sporulation. The sporulation-specific bPBP, SpoVD, is important for synthesizing the asymmetric division septum and spore cortex peptidoglycan during sporulation in the pathogen *Clostridioides difficile*. Although SpoVD catalytic activity is essential for cortex synthesis, we show that it is unexpectedly dispensable for SpoVD to mediate asymmetric division. The dispensability of SpoVD's catalytic activity requires the presence of its SEDS partner, SpoVE, and is facilitated by the catalytic activity of another sporulation-specific bPBP, PBP3. Our data further suggest that PBP3 interacts with components of the asymmetric division machinery, including SpoVD. These findings suggest a possible mechanism by which bPBPs can be functionally redundant in diverse bacteria and facilitate antibiotic resistance.

Introduction

Peptidoglycan (PG) synthesis is an essential driver of the morphological changes required for bacterial growth and division. The final steps of this crucial process include glycosyltransfer reactions that polymerize the glycan strands and transpeptidation reactions that crosslink the peptide sidechains between the strands (Egan et al., 2020; Rohs & Bernhardt, 2021). These enzymatic reactions require the activities of high-molecular-weight (HMW) Penicillin-binding proteins (PBPs) that are divided into two classes based on their catalytic ability: Class A PBPs (aPBP) are bifunctional enzymes capable of both glycosyltransferase and transpeptidase activities, while Class B PBPs are monofunctional transpeptidases (Goffin & Ghuysen, 1998; Sauvage et al., 2008). Since crosslinking of PG is essential in almost all bacteria, inhibiting PBP transpeptidase activity is typically lethal to bacterial cells. Consequently, beta-lactam antibiotics such as penicillin that inhibit PBPs by covalently bonding to the catalytic serine residue in their transpeptidase domain are some of the most successful and widely used antibiotics (Zapun et al., 2008). As such, identifying factors that confer resistance to beta-lactam antibiotics and determining their mechanism of action has been an area of significant interest.

One mechanism through which bacteria achieve resistance against beta-lactam antibiotics is by inducing the expression of PBPs with lowered binding affinities for specific beta-lactams. Most bacteria encode multiple PBPs that are specialized for specific cellular processes; some PBPs are essential, while others can be functionally redundant (Goffin & Ghuysen, 1998; Sauvage et al., 2008). Essential PBPs typically function as core components of highly conserved multiprotein complexes that drive cell wall synthesis during growth and division. The divisome is the essential complex responsible for driving septal PG synthesis through the activities of a bPBP transpeptidase that is partnered with a cognate glycosyltransferase, the latter of which is a member of the shape, elongation, division, and sporulation (SEDS) protein family (Cameron & Margolin, 2024; Rohs & Bernhardt, 2021; Taguchi et al., 2019). The elongasome is the multiprotein complex responsible for driving cell elongation in rod-shaped bacteria through the action of a distinct SEDS-bPBP pair (Emami et al., 2017; Meeske et al., 2015; Rohs & Bernhardt, 2021; Sjodt et al., 2020). Notably, these SEDS-bPBP pairs are highly specific because the bPBP acts as a selective allosteric activator of its cognate SEDS family glycosyltransferase activity (Shlosman et al., 2023; Sjodt et al., 2020).

66 Endospore-forming bacteria typically encode an additional SEDS-bPBP complex that is
67 responsible for driving the morphological changes required for spore formation (Galperin et al.,
68 2012, 2022; Shrestha et al., 2023; Tan & Ramamurthi, 2014). Sporulation begins with the
69 formation of a polar division septum close to one cell pole in a process called asymmetric
70 division. In *Bacillus subtilis*, asymmetric division is driven by the same SEDS-bPBP pair that
71 mediates cell division during vegetative growth (Barák et al., 2019; Khanna et al., 2020). In
72 contrast, we recently showed that the spore-forming pathogen *Clostridioides difficile* lacks a
73 canonical division-associated SEDS-bPBP pair for driving septal PG synthesis and instead uses
74 an aPBP as the major PG synthase during vegetative cell division (Shrestha et al., 2023). In
75 further contrast with *B. subtilis,* the sporulation-specific SEDS-bPBP pair SpoVE-SpoVD is an
76 important driver of septal PG synthesis during asymmetric division in *C. difficile*. Although the
77 role of SpoVE-SpoVD function during asymmetric division may be restricted to *C. difficile* and
78 other clostridial organisms, genes encoding SpoVE and SpoVD can be found in almost all spore
79 formers (Galperin et al., 2012, 2022). In both *B. subtilis* and *C. difficile*, SpoVE and SpoVD are
80 essential for the synthesis of the spore cortex, a thick layer of modified PG that surrounds and
81 protects the spore core (Henriques et al., 1992; Yanouri et al., 1993; Daniel et al., 1994; Shrestha
82 et al., 2023; Alabdali et al., 2021; Srikhanta et al., 2019). Thus, SpoVE and SpoVD are important
83 for synthesizing PG during two distinct stages of spore formation in *C. difficile*.
84 While a previous study showed that SpoVD's catalytic activity is essential for spore
85 formation in *C. difficile* (Alabdali et al., 2021), in this study, we surprisingly observe that SpoVD
86 catalytic activity is largely dispensable for mediating asymmetric division despite being essential
87 for synthesizing the cortex layer. Prior analyses of a catalytic mutant of a divisome-associated
88 bPBP, PBP2b$_{Bs}$, in *B. subtilis* provide a possible mechanism for explaining this observation. In *B.*
89 *subtilis*, the catalytic activity of PBP2b$_{Bs}$ is dispensable (Sassine et al., 2017) because a second
90 bPBP, PBP3$_{Bs}$, can supply the transpeptidase activity during septal PG synthesis. Since the gene
91 encoding PBP2b$_{Bs}$ is essential, presumably because the PBP2b$_{Bs}$ protein is required to
92 allosterically activate the glycosyltransferase activity of its SEDS binding partner, FtsW, these
93 observations highlight that PBP3$_{Bs}$ cannot complement all the roles fulfilled by the catalytically
94 inactive PBP2b$_{Bs}$. Notably, PBP3$_{Bs}$ is also important for resistance against certain beta-lactams,
95 since it has lower affinities for them compared to PBP2b$_{Bs}$ (Sassine et al., 2017). While these

observations highlight the importance of catalytic redundancies between PBPs, the molecular mechanisms behind this phenomenon remain unclear.

Here, we explore the role of SpoVD catalytic activity during asymmetric division in *C. difficile*. Our findings suggest that the ability of a catalytically inactive SpoVD to support septal PG synthesis during asymmetric division requires the presence of its SEDS partner SpoVE and is facilitated in part by another sporulation-specific bPBP, PBP3. Furthermore, we provide evidence suggesting that PBP3 interacts with components of the asymmetric division machinery, including SpoVD. These findings suggest a possible mechanism for how bPBPs in diverse bacteria can be functionally redundant and promote antibiotic resistance.

Results

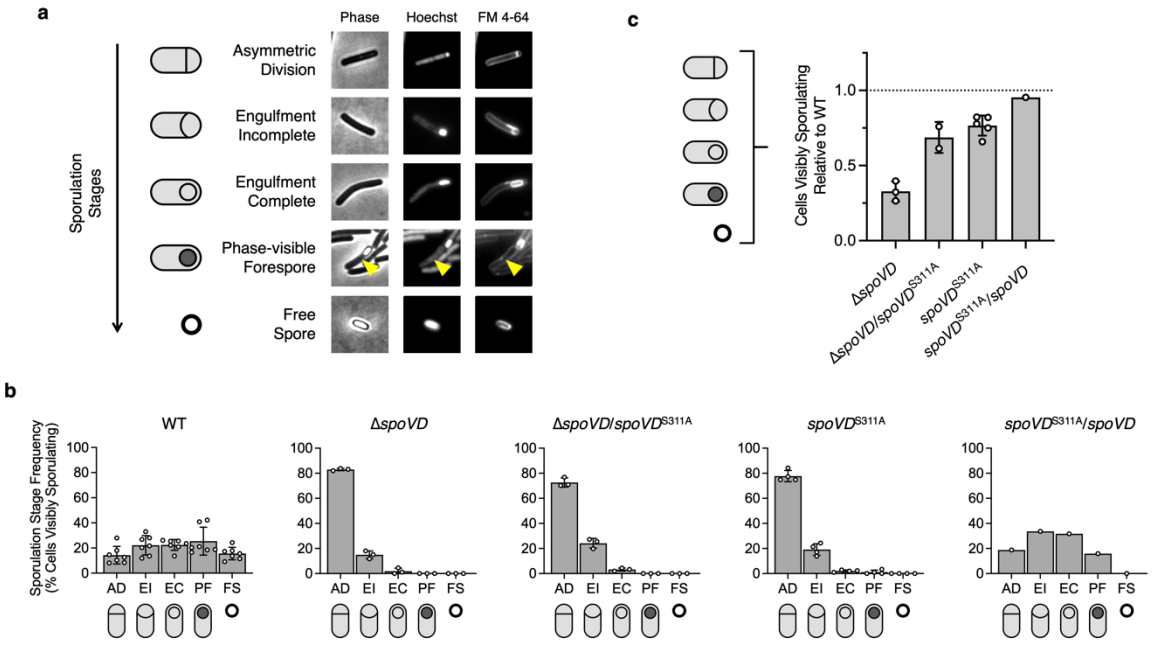

Fig. 1 | SpoVD catalytic activity is partially dispensable for its function during asymmetric division. **a** Cytological profile of individual cells representing each of the five morphological stages of sporulation as indicated. Representative phase-contrast and fluorescence micrographs are WT cells sampled from sporulation-inducing 70:30 plates after 18 of growth. The nucleoid was stained using Hoechst, and the cell membrane was stained using FM4-64. Cells undergoing asymmetric division (AD) have a flat polar septum; cells undergoing engulfment (EI) have a curved polar septum; cells that have completed engulfment (EC) exhibit bright-membrane staining around a fully engulfed forespore; phase-visible forespores (PF) are visible as phase-dark or phase-bright forespores associated with the mother cell (yellow arrow); mature free spores (FS) are observable as independent phase-bright particles. **b, c** Quantification of the cytological profiling of cells sampled from sporulation-inducing plates after 20-22 hours of growth. White circles

120 indicate data from each replicate, bars indicate average means, and error bars indicate standard deviation.
121 >1,000 total cells and >100 visibly sporulating cells per sample. **b** shows the distribution of visibly
122 sporulating cells among the indicated stages of sporulation. **c** shows the proportion of cells that complete
123 and progress beyond asymmetric division, i.e., all visibly sporulating cells, as a percentage of the total cells
124 profiled. Note that the data is normalized to WT (dotted line).
125

126 *SpoVD catalytic mutant is defective in cortex synthesis but not in asymmetric division*

127 Given that the catalytic activity of the division-specific bPBP in *B. subtilis* is not essential for its
128 role in cell division (Sassine et al., 2017), we speculated that the catalytic activity of SpoVD
129 might be similarly dispensable during asymmetric division in *C. difficile*. SpoVD retains the
130 SXXK active-site motif that is highly conserved among bPBPs. To abolish the catalytic activity
131 of SpoVD, we introduced an alanine substitution at the nucleophilic serine residue ($SpoVD_{S311A}$).
132 Consistent with a prior study (Alabdali et al., 2021), *C. difficile* strains with a catalytically
133 inactive SpoVD failed to produce heat-resistant spores (**Figure S1**). Importantly, this phenotype
134 was observed when $spoVD_{S311A}$ was expressed from an ectopic chromosomal locus
135 ($\Delta spoVD/spoVD_{S311A}$) or the native locus ($spoVD_{S311A}$) (**Figure S1**). Furthermore, the levels of
136 SpoVD present in these strains upon sporulation induction were found to be similar to wild-type
137 (WT) by western blot analysis (**Figure S2**).
138 To further define the role of SpoVD catalytic activity during spore formation, we
139 evaluated the ability of the SpoVD catalytic mutant strains to progress through the different
140 morphological stages of sporulation by cytologically profiling sporulating cells (**Figure 1a**)
141 (Nonejuie et al., 2013; Pogliano et al., 1999). Similar to the *spoVD* deletion strain, *spoVD*
142 catalytic mutant strains failed to produce phase-visible spores, indicating that they have defects
143 in cortex synthesis (**Figure 1b**). Furthermore, the distribution of sporulating cells among
144 different stages was similar between the strains, with most cells being stalled at the asymmetric
145 division stage and relatively few cells completing engulfment (**Figure 1b**). To specifically
146 quantify the effects on asymmetric division, we calculated the proportion of cells that showed
147 morphological signs of sporulation in the cytological profiling i.e., cells that progressed beyond
148 asymmetric division, as a percentage of all cells. These analyses revealed that, relative to WT,
149 $\Delta spoVD/spoVD^{S311A}$ and $spoVD^{S311A}$ cells complete asymmetric division at significantly higher
150 frequencies compared to $\Delta spoVD$ cells, with ~30% of $\Delta spoVD$ cells completing asymmetric
151 division and ~70% of $\Delta spoVD/spoVD^{S311A}$ and $spoVD^{S311A}$ cells completing asymmetric division

(**Figure 1c**). Since we have previously shown that the decreased frequency of Δ*spoVD* cells with visible signs of sporulation reflects a defect in asymmetric division rather than sporulation initiation (Shrestha et al., 2023), these results suggest that SpoVD function during asymmetric division is only partially dependent on its catalytic activity. Surprisingly, while we were able to complement the defects in asymmetric divison of the catalytic mutant strains by expressing a wild-type copy of *spoVD* from an ectopic locus (**Figure 1b, 1c**), this strain was unable to form mature phase-bright spores (**Figure S1, 1b**). This suggests that the catalytically inactive SpoVD has a dominant negative phenotype specifically for the defect in cortex synthesis.

The SpoVD catalytic mutant requires its SEDS partner, SpoVE

Since previous studies suggest that bPBPs are needed to allosterically activate the glycosyltransferase activity of their cognate SEDS family glycosyltransferases (Shlosman et al., 2023; Sjodt et al., 2020; Taguchi et al., 2019), we tested if the ability of SpoVD^{S311A} to support asymmetric division requires its SEDS partner SpoVE. To this end, we created a *spoVD*^{S311A}Δ*spoVE* strain by introducing the catalytic mutant variant of *spoVD* into the native locus of a Δ*spoVD*Δ*spoVE* strain. As expected, this strain failed to form heat-resistant spores (**Figure 2**). Cytological profiling of sporulating cells revealed that *spoVD*^{S311A}Δ*spoVE* cells complete and progress beyond asymmetric division at a significantly lower frequency (~25%) than WT or *spoVD*^{S311A} cells (100% and ~75%, respectively). Thus, the phenotype of *spoVD*^{S311A}Δ*spoVE* cells is similar to that of Δ*spoVD* and Δ*spoVE* cells (**Figure 2**). Since we previously showed that SpoVD levels are unaffected by loss of SpoVE (Shrestha et al., 2023), we conclude that the function of SpoVD^{S311A} during asymmetric division requires SpoVE.

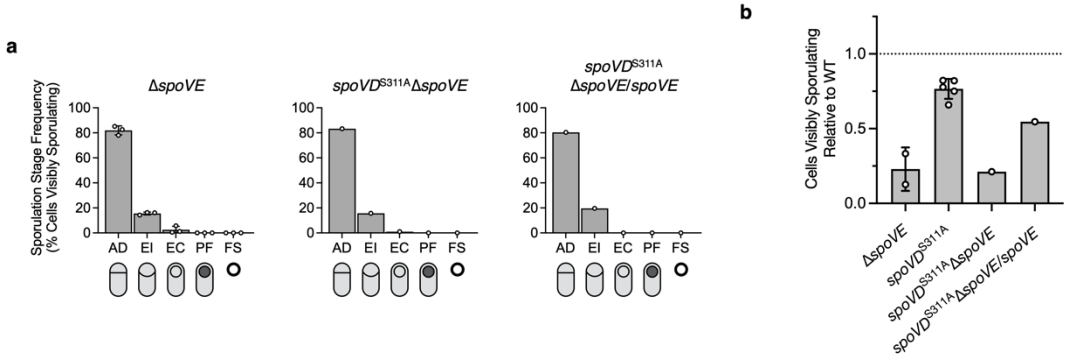

Fig. 2 | The catalytically inactive SpoVD requires its SEDS partner, SpoVE, to facilitate asymmetric division. a, b Quantification of the cytological profiling of cells sampled from sporulation-inducing plates after 20-22 hours of growth. White circles indicate data from each replicate, bars indicate the average mean, and error bars indicate standard deviation. >1,000 total cells and >100 visibly sporulating cells per

178 sample. **a** shows the distribution of visibly sporulating cells among the indicated stages of sporulation.
179 See Figure 1b for the distribution of WT cells. AD, Asymmetric Division; EI, Engulfment Initiated; EC,
180 Engulfment Completed; PF, Phase bright/dark Forespore; FS, Free Spore. **b** shows the proportion of cells
181 that complete and progress beyond asymmetric division, i.e., all visibly sporulating cells, as a percentage
182 of the total cells profiled. Note that the data is normalized to WT (dotted line).

183

184 *An additional non-essential bPBP, PBP3, is involved in sporulation*

185 Next, we wondered if *C. difficile* encodes an additional sporulation-specific bPBP that can cross-
186 link septal PG synthesis in the absence of SpoVD catalytic activity similar to the functional
187 redundancy observed between division-specific bPBPs in *B. subtilis* (Sassine et al., 2017). Most
188 *C. difficile* strains encode three bPBPs (Isidro et al., 2017, 2018): one sole essential bPBP, PBP2,
189 which primarily functions during cell elongation, and two other bPBPs, SpoVD and PBP3, which
190 are dispensable for vegetative growth (Shrestha et al., 2023). PBP3 is a close homolog of SpoVD
191 containing a similar domain composition apart from the C-terminal PASTA (PBP And
192 Serine/Threonine kinase Associated) domain carried by SpoVD (**Figure 3a**). Both PBP3 and
193 SpoVD have an N-terminal transmembrane section followed by PBP dimerization and
194 transpeptidase domains.

195 We considered PBP3 to be a likely candidate for providing functional redundancy to
196 SpoVD during asymmetric division for several reasons. First, previous studies suggest that the
197 expression of *pbp3* (locus *cd630_12290* in the strain used in this study) is upregulated at the
198 onset of sporulation in a manner similar to *spoVD* expression (Fimlaid et al., 2013; Saujet et al.,
199 2013). Second, we previously showed that individual deletions of *spoVD* or *pbp3* do not affect
200 the growth rate of vegetative cells, suggesting that SpoVD and PBP3 play sporulation-specific
201 roles (Shrestha et al., 2023). This agrees with our western blot analysis showing that SpoVD and
202 PBP3 are produced under sporulation-inducing conditions in a manner dependent on the
203 presence of the master transcriptional regulator of sporulation, Spo0A **(Figure 3).** Taken together
204 with prior transcriptomic studies (Fimlaid et al., 2013; Saujet et al., 2013), which similarly show
205 Spo0A-dependent induction of *pbp3* and *spoVD* transcription, these observations demonstrate
206 that both proteins are produced prior to asymmetric division. Furthermore, the Δ*pbp3* strain
207 forms heat-resistant spores ~2-fold less efficiently than WT, a modest defect that can be
208 complemented by expressing *pbp3* from an ectopic chromosomal locus (**Figure 3c**). This result
209 is consistent with a prior transposon mutagenesis screen, which identified *pbp3* to be important

for sporulation (Dembek et al., 2015). Since phase-contrast microscopy of sporulating cells revealed that the Δ*pbp3* mutant forms phase-bright forespores and free spores, and thus capable of assembling the spore cortex, our data indicate that PBP3 is dispensable for this process unlike SpoVD (**Figure 3d**). These results suggest that PBP3 is a sporulation-specific factor that is involved in, but not essential for, the formation of mature spores in *C. difficile*.

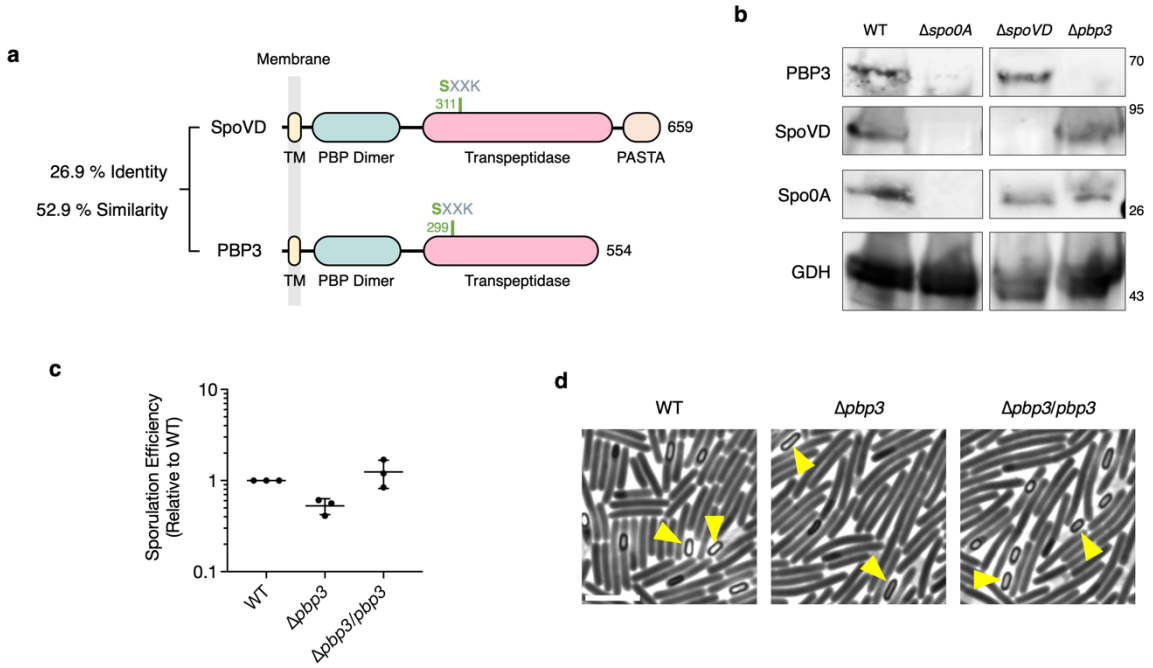

Fig. 3 | PBP3 is a sporulation-specific bPBP involved in spore formation. a Protein schematic comparing SpoVD and PBP3. Functional domains and catalytic sites were predicted using HMMER. TM, transmembrane domain; PASTA, penicillin-binding protein and serine/threonine kinase-associated domain. **b** Western blot showing the levels of the SpoVD, PBP3, Spo0A, and GDH in WT, Δ*spo0A*, Δ*spo0A*, and Δ*pbp3* cells sampled from sporulation-inducing plates after ~20 hours of growth. SpoVD and PBP3 are not detected in the Δ*spo0A* strain, which cannot initiate sporulation. Levels of the constitutively produced glutamate dehydrogenase (GDH) are shown as a control. **c** Efficiency of heat-resistant spore formation (sporulation efficiency) of the *pbp3* mutant and complemented strains relative to WT. Means with standard deviation are indicated. Cells were collected from sporulation-inducing 70:30 plates ~20-22 hours after inoculation. Data from three independent experiments. **d** Representative phase-contrast micrographs of WT, *pbp3* mutant, and complemented cells collected from sporulation-inducing 70:30 plates after ~20 hours of growth. Examples of phase-bright spores are indicated by yellow arrows. Scale bar, 5 µm.

PBP3 can partially substitute for the loss of SpoVD catalytic activity during asymmetric division

To test if PBP3 provides redundancy to SpoVD catalytic activity during asymmetric division, we analyzed the ability of Δ*pbp3* cells to complete asymmetric division in the context of WT and

catalytically inactive SpoVD variants. Cells lacking PBP3 completed asymmetric division at WT levels in the presence of WT SpoVD (**Figure 4b**). The distribution of sporulating Δ*pbp3* cells among the different sporulation stages was also similar to WT (**Figure 4a**). Importantly, in a SpoVD catalytic mutant background, cells lacking PBP3 completed asymmetric division at a lower rate when compared to WT or *spoVD*^{S311A} cells (**Figure 4b**). However, the proportion of *spoVD*^{S311A}Δ*pbp3* cells that complete asymmetric division was higher compared to Δ*spoVD* cells (**Figure 4b**), suggesting that PBP3 transpeptidase only partially accounts for the ability of the catalytically dead SpoVD to support asymmetric division. To establish if this partial redundancy requires the transpeptidase activity of PBP3, we introduced *pbp3*^{S299A}, which encodes a catalytically inactive PBP3 in an ectopic chromosomal locus of a *spoVD*^{S311A} Δ*pbp3* strain. Cytological profiling of the *spoVD*^{S311A} Δ*pbp3*/*pbp3*^{S299A} strain revealed that these cells complete asymmetric division at a similar rate to the *spoVD*^{S311A} strain (**Figure 4**). Hence, our data suggest that the transpeptidase activity of PBP3 provides partial functional redundancy to SpoVD catalytic activity specifically during asymmetric division.

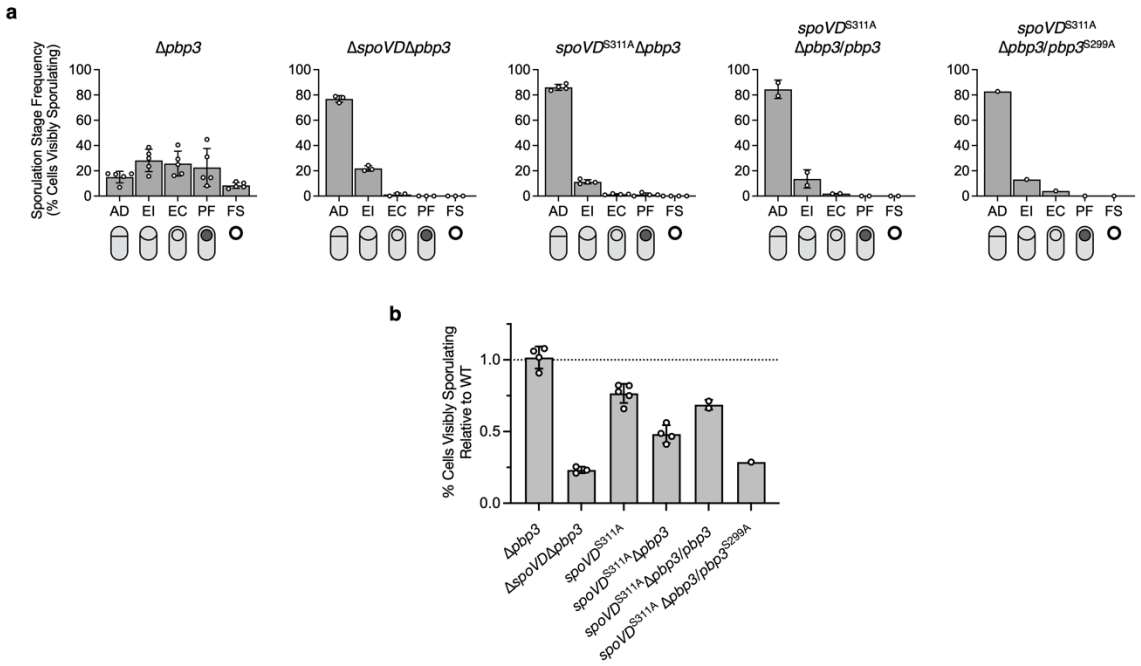

Fig. 4 | PBP3 catalytic activity plays a partially redundant role to SpoVD catalytic activity during asymmetric division. a, b Quantification of the cytological profiling of cells sampled from sporulation-inducing plates after 20-22 hours of growth. White circles indicate data from each replicate, bars indicate average means, and error bars indicate standard deviation. >1,000 total cells and >100 visibly sporulating cells per sample. **a** shows the distribution of visibly sporulating cells among the indicated stages of

sporulation. See **Figure 1b** for the distribution of WT cells. AD, Asymmetric Division; EI, Engulfment Initiated; EC, Engulfment Completed; PF, Phase bright/dark Forespore; FS, Free Spore. **b** shows the proportion of cells that complete and progress beyond asymmetric division, i.e., all visibly sporulating cells, as a percentage of the total cells profiled. Note that the data is normalized to WT (dotted line).

PBP3 may interact with PG-synthesizing enzymes and components of the polar divisome

Our previous study suggests that SpoVD likely functions as part of the polar divisome to synthesize septal PG during asymmetric division (Shrestha et al., 2023). The partial redundancy between PBP3 and SpoVD catalytic activities during asymmetric division observed here suggests that PBP3 might be recruited to this machinery during this process. To test whether PBP3 interacts with polar divisome, we conducted bacterial two-hybrid assays to probe pairwise interactions between PBP3 and various components of this complex. In addition to SpoVD and SpoVE, we explored interactions with three additional proteins, FtsL, FtsQ, and FtsB (also known as FtsL, DivIB, and DivIC in some Firmicutes), which form a highly-conserved divisome sub-complex that regulates PG synthase activity during cell division in other bacteria (Levin & Losick, 1994; Daniel et al., 1998; Katis & Wake, 1999; Tsang & Bernhardt, 2015; Marmont & Bernhardt, 2020; Shrestha et al., 2023). Our data suggests that PBP3 can interact with various components of the polar divisome, including SpoVD, SpoVE, and FtsQ (**Figure 5a**). As controls, we also probed interactions between PBP3 and all other PBP and SEDS-family proteins encoded by *C. difficile*. Surprisingly, our analysis indicates that PBP3 also interacts with PBP2 and PBP1 (**Figure 5a**), which primarily function during vegetative cell elongation and division, respectively, but likely also play important roles during spore formation. Although surprising, this suggests that PBP3 may be able to supplement the transpeptidation activities of other PBPs in *C. difficile* during spore formation. Overall, our data implies that PBP3 is recruited to the polar divisome complex through direct interactions with its components (**Figure 5b**).

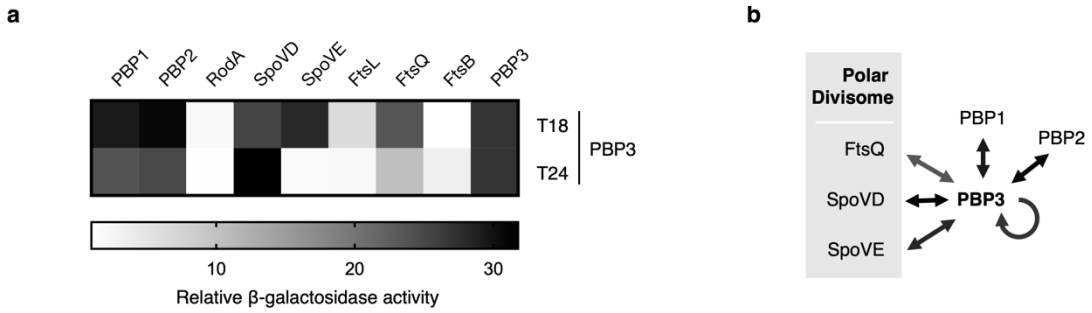

Fig. 5 | PBP3 interacts with multiple components of the polar divisome. a Bacterial two-hybrid analysis of interactions between PBP3 and other PG synthases or components of the polar divisome. The

β-galactosidase activity was normalized to the negative control. N-terminal T18 or T24 fusion to PBP3 was paired with reciprocal N-terminal fusions to the indicated proteins. Data from three technical replicates. **B** The schematic shows detected interactions from (a) where arrows are colored according to the amount of maximum β-galactosidase activity detected. Components of the predicted polar divisome are indicated.

Endospore-forming bacteria typically encode multiple additional bPBPs compared to non-sporulating bacteria

Since *B. subtilis* also encodes multiple sporulation-specific class B PBPs, we wondered whether functional redundancies between sporulation-specific bPBPs might be more broadly conserved in endospore-forming bacteria. To this end, we compared the numbers of SEDS and bPBP enzymes encoded in the genomes of non-sporulating and sporulating Firmicutes, the sole bacterial phyla with endospore-forming members. Our analyses revealed that sporulating bacteria typically encode a higher number of bPBPs compared to non-sporulating bacteria (**Figure 6**). In sporulating organisms, the number of encoded bPBPs often exceeds the number of encoded SEDS (214/328; 65%), while only a small minority encode more SEDS proteins than bPBPs (20/328; 6%). Furthermore, a higher percentage of non-sporulating organisms encode equal numbers of SEDS and bPBP genes (80%). These observations are consistent with the prevalence of additional sporulation-specific PG synthases in spore formers and suggest that redundancy in bPBP activity is likely widespread in these organisms.

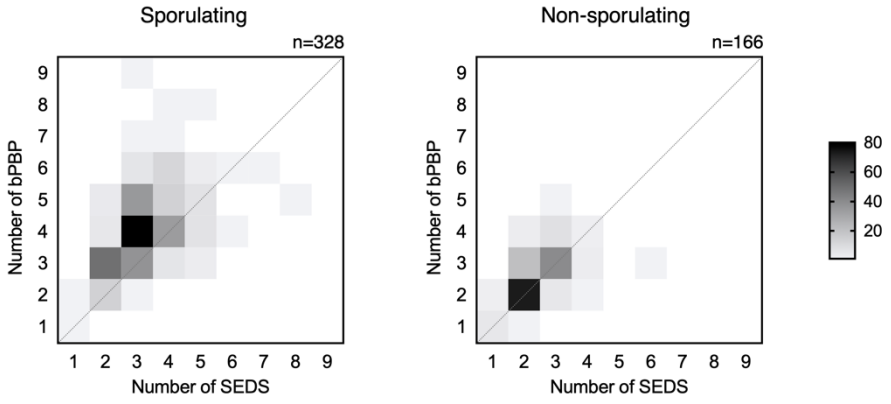

Fig. 6 | Prevalence of bPBP and SEDS enzymes in Firmicutes. Heatmaps showing the distribution of class B penicillin-binding protein (bPBP) and SEDS protein numbers encoded in the genomes of sporulating (n=328) and non-sporulating (n=166) Firmicutes organisms. Sporulation ability was inferred by the presence of broadly conserved sporulation-specific genes *spo0A* and *spoIIE* in the genome. The dataset is composed of 494 diverse Firmicutes organisms as reported in Shrestha *et al*., 2023.

311 **Discussion**

312

313 While most bacteria encode multiple bPBPs that perform specialized roles during specific
314 cellular processes, some bPBPs can play redundant roles that are important for resistance against
315 environmental stresses. Our understanding of these compensatory mechanisms and their
316 prevalence, however, remains incomplete. Here, we reveal that the catalytic activity of SpoVD in
317 *C. difficile* is partially dispensable for its function during the synthesis of the polar septum
318 (**Figure 1)**. Furthermore, we demonstrate that a previously uncharacterized sporulation-specific
319 bPBP, PBP3, is important for this dispensability since it can partially substitute for SpoVD's
320 catalytic activity during asymmetric division (**Figures 3, 4**). Finally, our data suggests that PBP3
321 likely functions as a part of the polar divisome, which mediates asymmetric division, via direct
322 interactions with its components (**Figure 5**).

323 Functional redundancies between PBPs have important implications for cellular
324 adaptation to environmental stresses and resistance against antibiotics targeting PG
325 transpeptidation. Redundancies between aPBPs have been described in *Escherichia coli* (Mueller
326 et al., 2019), *B. subtilis,* and *Streptococcus pneumoniae* (Mitchell et al., 2023), where distinct
327 aPBPs are specialized to respond to changes in environmental pH but can also play redundant
328 roles in certain conditions. Similarly, niche specialization of different bPBPs was observed in
329 *Salmonella enterica*, which encodes two division-specific and two elongation-specific bPBPs
330 that are functionally specialized for extracellular or intracellular conditions (Castanheira et al.,
331 2017, 2020). Furthermore, as described above, functional redundancy in bPBP activities during
332 cell division in *B. subtilis* lowers its sensitivity to certain β-lactams (Sassine et al., 2017). Given
333 that different bPBPs have distinct binding affinities to β-lactams, it is thought that typically
334 dispensable bPBPs can facilitate resistance by providing transpeptidation activity with an
335 inherently low affinity to the inhibitor when an essential bPBP is targeted. This is supported by
336 studies in methicillin-resistant *Staphylococcus aureus* (MRSA), where strains that have acquired
337 an additional low-affinity bPBP display lower sensitivity to certain β-lactams (Hartman &
338 Tomasz, 1984; Wielders et al., 2002). Similarly, a typically non-essential *Enterococcus faecalis*
339 bPBP with low reactivity to cephalosporins provides functional redundancy to the primary
340 division-associated bPBP during cephalosporin treatment (Djorić et al., 2020; Nelson et al.,
341 2024).

342 While the molecular mechanisms enabling redundancies between bPBPs remain unclear,
343 these observations suggest a few different possibilities. In the case of *S. enterica*, the two
344 division-specific bPBPs appear to function independently since neither bPBP requires the
345 presence of the other to function in their respective niche (Castanheira et al., 2017). In contrast,
346 the functional redundancy reported between PBP3$_{Bs}$ and PBP2b$_{Bs}$ in *B. subtilis* when the catalytic
347 activity of the primary division-specific bPBP, PBP2b$_{Bs}$ is inactivated depends on the presence of
348 the catatlytically inactivated PBP2b$_{Bs}$ protein (Sassine et al., 2017). Since SEDS-bPBP pairs are
349 thought to be comprised of cognate partners whose activities are coordinated by and require their
350 interaction (Shlosman et al., 2023; Sjodt et al., 2020; Taguchi et al., 2019), it is likely that the
351 requirement of PBP2b$_{Bs}$ is dictated by the structural role it plays in interacting with and
352 stimulating the glycosyltransferase activity of the division-specific SEDS protein. This is
353 consistent with an *in vitro* study, which showed that a catalytically inactive form of a bPBP can
354 support PG polymerization by its SEDS partner (Taguchi et al., 2019). Furthermore, the
355 redundancy observed in *E. faecalis* is suggested to require direct interaction between the two
356 bPBPs within the larger divisome complex (Nelson et al., 2024). In contrast, since the two
357 division-specific bPBPs in *S. enterica* can function independently from one another, it is possible
358 that either enzyme can interact with the division-specific SEDS glycosyltransferase (Castanheira
359 et al., 2017).
360 Since the activity of *C. difficile* PBP3 during asymmetric division requires the presence
361 of SpoVD (**Figure 1**), redundancy between these sporulation-specific bPBPs is analogous to the
362 catalytic redundancy observed between division-specific bPBPs in *B. subtilis*. We speculate that
363 the requirement for SpoVD, even when catalytically inactive, is due to SpoVD's function in
364 allosterically activating SpoVE activity. In addition, SpoVD may play a crucial role in the
365 formation and function of the polar divisome complex. Importantly, our results show that PBP3
366 can interact with different members of the polar divisome, suggesting it may be recruited to this
367 complex during asymmetric division. The active recruitment of functionally redundant bPBPs to
368 the divisome is consistent with the finding that septal PG synthesis is a highly controlled process
369 involving various localization and regulatory mechanisms (Egan et al., 2020). Moreover, since
370 functional redundancies appear to be constrained to distinct bPBP pairs and specialized for
371 specific cellular processes, it is unlikely that a functionally redundant bPBP functions
372 independently. Due to the requirement for SpoVD, we speculate that PBP3 is likely recruited as

373 an additional factor rather than replacing SpoVD in the polar divisome complex. However,
374 confirmation and characterization of the mechanisms and factors facilitating this recruitment
375 require further study. Since bacterial two-hybrid assays only probe pairwise interactions in a non-
376 native system, it will be important to define these interactions in the native context, including all
377 components of the polar divisome.

378 It remains unclear why SpoVD catalytic activity is largely dispensable for during
379 asymmetric division but essential for cortex synthesis. It is possible that cortex synthesis
380 involves SpoVE-SpoVD to function as part of a larger PG synthetic complex, similar to the
381 divisome and elongasome. Since SpoVE-SpoVD function during this process requires their
382 specific localization to the forespore, it is likely that other factors are involved in their regulation.
383 It is, therefore, possible that the inability of PBP3 to functionally compensate for the loss of
384 SpoVD catalytic activity during cortex synthesis results from its decreased affinity for these
385 unknown factors. Another possibility is that the amount of crosslinking required is higher than
386 PBP3 is able to supplement during this process. This is consistent with our finding that an
387 ectopically expressed *spoVD* is unable to alleviate the cortex synthesis defect observed upon
388 introducing the catalytic mutation in the native copy of *spoVD*. Thus, more research is required
389 to define the factors and mechanisms regulating SpoVE-SpoVD activity during cortex synthesis.

390 Finally, redundancy in bPBP activity is likely widespread among spore-forming bacteria
391 based on our finding that they typically encode multiple additional bPBPs, the number of which
392 often exceeds the number of SEDS glycosyltransferases encoded in the genome (**Figure 6**).
393 Defining specialized roles or redundancies between these enzymes requires further study and
394 may have important implications of the ability of these organisms to respond to environmental
395 and antibiotic stress. Interestingly, while most *C. difficile* strains carry five distinct HMW PBPs,
396 a study characterizing clinical strains identified an additional bPBP encoded by *Clostridium*
397 *difficile* ribotype 017 isolates (Isidro et al., 2017, 2018). Some of these isolates have a lower
398 sensitivity to the beta-lactam imipenem and carry mutations in the transpeptidase catalytic sites
399 of the division-associated PBP1 and elongation-associated PBP2. The additional bPBP encoded
400 by these strains, therefore, may additionally contribute to imipenem resistance by providing
401 functional redundancy to these enzymes or SpoVD, recapitulating the scenario observed in
402 MRSA strains. Taken together with our findings, these observations highlight the need to define

403 functional redundancies between PBPs in *C. difficile* and their possible roles in driving antibiotic
404 resistance of this important pathogen.

405 **Methods**

406 *C. difficile strain construction and growth conditions*

407 All *C. difficile* strains are derived from the 630Δ*erm* strain. Deletion and complementation
408 strains were constructed in a Δ*pyrE* background strain using *pyrE*-based allele-coupled exchange
409 as previously described (Ng et al., 2013). All strains used in the study are reported in Table 1.
410 Strains were grown at 37°C under anaerobic conditions using a gas mixture containing 85% N_2,
411 5% CO_2, and 10% H_2.

412 *E. coli strain constructions*

413 Table 2 lists all plasmids used in the study, with links to plasmid maps containing all primer
414 sequences used for cloning. Plasmids were cloned via Gibson assembly, and cloned plasmids
415 were transformed into *E. coli* (DH5α or XL1-Blue strains). All plasmids were confirmed by
416 sequencing the inserted region. Confirmed plasmids were transformed into the *E. coli*
417 HB101(pRK24) strain for conjugation with *C. difficile* when needed. All *E. coli* HB101 strains
418 used for conjugation are also listed in Table 2.

419 *Plate-based sporulation assays*

420 For assays requiring sporulating cells, cultures were grown to early stationary phase, back-
421 diluted >25-fold into BHIS, and grown until they reached exponential phase (OD_{600} between
422 0.35 and 0.75). 120 µL of exponentially growing cells were spread onto 70:30 (70% SMC media
423 and 30% BHIS media) agar plates (40 mL media per plate). After 18-22 hours of growth,
424 sporulating cells were collected into phosphate-buffered saline (PBS), and sporulation levels
425 were visualized by phase-contrast microscopy as previously described (Pishdadian et al., 2015).

426 *Heat resistance assay*

427 Heat-resistant spore formation was measured 20-22 hours after sporulation induction on 70:30
428 agar plates by resuspending sporulating cells in PBS, dividing the sample into two, heat-treating
429 one of the samples at 60˚C for ~30 min, and comparing the colony-forming units (CFUs) in the
430 untreated sample to the heat-treated sample (Fimlaid et al., 2015). Heat-resistance efficiencies

431 represent the average ratio of heat-resistant CFUs to total CFUs for a given strain relative to the
432 average ratio for the wild-type strain.

433 *Western blot analysis*

434 Samples were collected 18-22 hours after sporulation induction on 70:30 agar plates and
435 processed for immunoblotting. Sample processing involved multiple freeze-thaws in PBS
436 followed by the addition of EBB buffer (9 M urea, 2 M thiourea, 4% SDS, 2 mM b-
437 mercaptoethanol), boiling, pelleting, resuspension, and boiling again before loading on a gel. All
438 proteins were resolved using 4–15% precast polyacrylamide gels (Bio-Rad) and transferred to
439 polyvinylidene difluoride membranes, which were subsequently probed with rabbit (anti-PBP3
440 and anti-SpoVD (Shrestha et al., 2023); both at 1:1,000 dilution), mouse (anti-Spo0A (Fimlaid et
441 al., 2013) at 1:1,000 dilution) and chicken (anti-GDH at 1:5,000 dilution) polyclonal primary
442 antibodies, and anti-rabbit (IR800 or IR680), anti-mouse (IR680) and anti-chicken (IR800)
443 secondary antibodies (LI-COR Biosciences, 1:20,000 dilution). Blots were imaged using a LiCor
444 Odyssey CLx imaging system. The results shown are representative of multiple experiments.

445 *Bacterial two-hybrid analyses*

446 Bacterial adenylate cyclase two-hybrid (BACTH) assays were conducted as previously described
447 (Karimova et al., 1998) using *E. coli* BTH101 cells. Briefly, BTH101 cells were transformed
448 with 100 ng of each plasmid and plated on LB agar plates supplemented with 50 µg/ml
449 kanamycin, 100 µg/ml Ampicillin, and 0.5 mM isopropyl β-D-thiogalactopyranoside (IPTG).
450 Plates were incubated for 64-68 hours at 30°C, and β-galactosidase activity was quantified in
451 Miller units as previously detailed (Dahlstrom et al., 2015). The β-galactosidase activity of cells
452 transformed with the empty pUT18C and pKT25 vectors was used as a negative control for
453 normalization.

454 *Cell labeling and microscopy*

455 Fluorescence microscopy was performed on sporulating cells using Hoechst 33342 (Molecular
456 Probes; 15 µg/mL) and FM4-64 (Invitrogen; 1 µg/mL) to stain nucleoid and membrane,
457 respectively. All samples for a given experiment were imaged from a single agar pad (1.5% low-
458 melting point agarose in PBS).

Phase-contrast images in **Figure 3** were obtained using a Zeiss Axioskop upright microscope with a 100× Plan-NEOFLUAR oil-immersion phase-contrast objective and a Hamamatsu C4742-95 Orca 100 CCD Camera. All other phase-contrast and fluorescence images were acquired using a Leica DMi8 inverted microscope with a 63× 1.4 NA Plan Apochromat oil-immersion phase-contrast objective, a high precision motorized stage (Pecon), and an incubator (Pecon) set at 37˚C. Excitation light was generated by a Lumencor Spectra-X multi-LED light source with integrated excitation filters. An XLED-QP quadruple-band dichroic beam-splitter (Leica) was used (transmission: 415, 470, 570, and 660 nm) with an external filter wheel for all fluorescent channels. FM4-464 was excited at 550/38 nm and emitted light was filtered using a 705/72 nm emission filter (Leica); Hoechst was excited at 395/40 nm and emitted light was filtered using a 440/40 nm emission filter (Leica). Emitted and transmitted light was detected using a Leica DFC 9000 GTC sCMOS camera. 1 to 2 µm z-stacks were taken when needed with 0.21 µm z-slices.

Images were acquired and exported using the LASX software without further processing. After export, images were processed using Fiji (Schindelin et al., 2012) to remove out-of-focus regions, and the best-focused z-planes for all channels were manually selected. Image scaling was adjusted to improve brightness and contrast for display and was applied equally to all images shown in a single panel. Visualization of quantified data and any associated statistical tests were performed using Prism 10 (GraphPad Software, San Diego, CA, USA).

Acknowledgments

We acknowledge the University of Vermont Microscopy Imaging Core for processing the samples and acquiring the images for all Transmission Electron Microscopy analyses. We are grateful to members of the Shen lab for helpful discussions and feedback on the project. The National Institute of Allergy and Infectious Diseases grant R01 AI122232 (to A.S.) and Burroughs Wellcome Fund for Investigators in Pathogenesis Award (to A.S.) provided funding for this work.

Author Contributions

S.S. and A.S. conceived the study. S.S., J.M.D., and M.M. performed and analyzed experiments. A.S. supervised the study. S.S. wrote the manuscript with input from the other authors. All authors reviewed and approved the manuscript.

493 **References**

494

495 Alabdali, Y. A. J., Oatley, P., Kirk, J. A., & Fagan, R. P. (2021). A cortex-specific penicillin-
496 binding protein contributes to heat resistance in *Clostridioides difficile* spores. *Anaerobe*,
497 *70*, 102379. https://doi.org/10.1016/j.anaerobe.2021.102379

498 Barák, I., Muchová, K., & Labajová, N. (2019). Asymmetric cell division during *Bacillus subtilis*
499 sporulation. *Future Microbiology*, *14*(4), 353–363. https://doi.org/10.2217/fmb-2018-
500 0338

501 Cameron, T. A., & Margolin, W. (2024). Insights into the assembly and regulation of the bacterial
502 divisome. *Nature Reviews Microbiology*, *22*(1), 33–45. https://doi.org/10.1038/s41579-
503 023-00942-x

504 Castanheira, S., Cestero, J. J., Rico-Pérez, G., García, P., Cava, F., Ayala, J. A., Pucciarelli, M.
505 G., & García-del Portillo, F. (2017). A Specialized Peptidoglycan Synthase Promotes
506 *Salmonella* Cell Division inside Host Cells. *mBio*, *8*(6), e01685-17.
507 https://doi.org/10.1128/mBio.01685-17

508 Castanheira, S., López-Escarpa, D., Pucciarelli, M. G., Cestero, J. J., Baquero, F., & García-del
509 Portillo, F. (2020). An alternative penicillin-binding protein involved in *Salmonella*
510 relapses following ceftriaxone therapy. *eBioMedicine*, *55*, 102771.
511 https://doi.org/10.1016/j.ebiom.2020.102771

512 Dahlstrom, K. M., Giglio, K. M., Collins, A. J., Sondermann, H., & O'Toole, G. A. (2015).
513 Contribution of Physical Interactions to Signaling Specificity between a Diguanylate
514 Cyclase and Its Effector. *mBio*, *6*(6), 10.1128/mbio.01978-15.
515 https://doi.org/10.1128/mbio.01978-15

516 Daniel, R. A., Drake, S., Buchanan, C. E., Scholle, R., & Errington, J. (1994). The *Bacillus*
517 *subtilis spoVD* gene encodes a mother-cell-specific penicillin-binding protein required for
518 spore morphogenesis. *Journal of Molecular Biology*, *235*(1), 209–220.
519 https://doi.org/10.1016/S0022-2836(05)80027-0

520 Daniel, R. A., Harry, E. J., Katis, V. L., Wake, R. G., & Errington, J. (1998). Characterization of
521 the essential cell division gene *ftsL*(*yIID*) of *Bacillus subtilis* and its role in the assembly
522 of the division apparatus. *Molecular Microbiology*, *29*(2), 593–604.
523 https://doi.org/10.1046/j.1365-2958.1998.00954.x

Dembek, M., Barquist, L., Boinett, C. J., Cain, A. K., Mayho, M., Lawley, T. D., Fairweather, N. F., & Fagan, R. P. (2015). High-throughput analysis of gene essentiality and sporulation in *Clostridium difficile*. *mBio*, *6*(2), e02383. https://doi.org/10.1128/mBio.02383-14

Djorić, D., Little, J. L., & Kristich, C. J. (2020). Multiple Low-Reactivity Class B Penicillin-Binding Proteins Are Required for Cephalosporin Resistance in Enterococci. *Antimicrobial Agents and Chemotherapy*, *64*(4), 10.1128/aac.02273-19. https://doi.org/10.1128/aac.02273-19

Egan, A. J. F., Errington, J., & Vollmer, W. (2020). Regulation of peptidoglycan synthesis and remodelling. *Nature Reviews. Microbiology*, *18*(8), 446–460. https://doi.org/10.1038/s41579-020-0366-3

Emami, K., Guyet, A., Kawai, Y., Devi, J., Wu, L. J., Allenby, N., Daniel, R. A., & Errington, J. (2017). RodA as the missing glycosyltransferase in *Bacillus subtilis* and antibiotic discovery for the peptidoglycan polymerase pathway. *Nature Microbiology*, *2*, 16253. https://doi.org/10.1038/nmicrobiol.2016.253

Fimlaid, K. A., Bond, J. P., Schutz, K. C., Putnam, E. E., Leung, J. M., Lawley, T. D., & Shen, A. (2013). Global Analysis of the Sporulation Pathway of *Clostridium difficile*. *PLoS Genetics*, *9*(8), e1003660. https://doi.org/10.1371/journal.pgen.1003660

Fimlaid, K. A., Jensen, O., Donnelly, M. L., Francis, M. B., Sorg, J. A., & Shen, A. (2015). Identification of a Novel Lipoprotein Regulator of *Clostridium difficile* Spore Germination. *PLOS Pathogens*, *11*(10), e1005239. https://doi.org/10.1371/journal.ppat.1005239

Galperin, M. Y., Mekhedov, S. L., Puigbo, P., Smirnov, S., Wolf, Y. I., & Rigden, D. J. (2012). Genomic determinants of sporulation in Bacilli and Clostridia: Towards the minimal set of sporulation-specific genes. *Environmental Microbiology*, *14*(11), 2870–2890. https://doi.org/10.1111/j.1462-2920.2012.02841.x

Galperin, M. Y., Yutin, N., Wolf, Y. I., Vera Alvarez, R., & Koonin, E. V. (2022). Conservation and Evolution of the Sporulation Gene Set in Diverse Members of the Firmicutes. *Journal of Bacteriology*, *204*(6), e00079-22. https://doi.org/10.1128/jb.00079-22

Goffin, C., & Ghuysen, J.-M. (1998). Multimodular Penicillin-Binding Proteins: An Enigmatic Family of Orthologs and Paralogs. *Microbiology and Molecular Biology Reviews*, *62*(4), 1079–1093.

555 Hartman, B. J., & Tomasz, A. (1984). Low-affinity penicillin-binding protein associated with
556 beta-lactam resistance in *Staphylococcus aureus*. *Journal of Bacteriology*, *158*(2), 513–
557 516. https://doi.org/10.1128/jb.158.2.513-516.1984
558 Henriques, A. O., de Lencastre, H., & Piggot, P. J. (1992). A *Bacillus subtilis* morphogene cluster
559 that includes *spoVE* is homologous to the mra region of *Escherichia coli*. *Biochimie*,
560 *74*(7–8), 735–748. https://doi.org/10.1016/0300-9084(92)90146-6
561 Isidro, J., Mendes, A. L., Serrano, M., O.Henriques, A., & Oleastro, M. (2017). Overview of
562 *Clostridium difficile* Infection: Life Cycle, Epidemiology, Antimicrobial Resistance and
563 Treatment. *Clostridium Difficile - A Comprehensive Overview*.
564 https://doi.org/10.5772/intechopen.69053
565 Isidro, J., Santos, A., Nunes, A., Borges, V., Silva, C., Vieira, L., Mendes, A. L., Serrano, M.,
566 Henriques, A. O., Gomes, J. P., & Oleastro, M. (2018). Imipenem Resistance in
567 *Clostridium difficile* Ribotype 017, Portugal. *Emerging Infectious Diseases*, *24*(4), 741–
568 745. https://doi.org/10.3201/eid2404.170095
569 Karimova, G., Pidoux, J., Ullmann, A., & Ladant, D. (1998). A bacterial two-hybrid system
570 based on a reconstituted signal transduction pathway. *Proceedings of the National*
571 *Academy of Sciences*, *95*(10), 5752–5756. https://doi.org/10.1073/pnas.95.10.5752
572 Katis, V. L., & Wake, R. G. (1999). Membrane-bound division proteins DivIB and DivIC of
573 *Bacillus subtilis* function solely through their external domains in both vegetative and
574 sporulation division. *Journal of Bacteriology*, *181*(9), 2710–2718.
575 https://doi.org/10.1128/JB.181.9.2710-2718.1999
576 Khanna, K., Lopez-Garrido, J., & Pogliano, K. (2020). Shaping an Endospore: Architectural
577 Transformations During *Bacillus subtilis* Sporulation. *Annual Review of Microbiology*,
578 *74*(1), 361–386. https://doi.org/10.1146/annurev-micro-022520-074650
579 Levin, P. A., & Losick, R. (1994). Characterization of a cell division gene from *Bacillus subtilis*
580 that is required for vegetative and sporulation septum formation. *Journal of Bacteriology*,
581 *176*(5), 1451–1459. https://doi.org/10.1128/jb.176.5.1451-1459.1994
582 Marmont, L. S., & Bernhardt, T. G. (2020). A conserved subcomplex within the bacterial
583 cytokinetic ring activates cell wall synthesis by the FtsW-FtsI synthase. *Proceedings of*
584 *the National Academy of Sciences*, *117*(38), 23879–23885.
585 https://doi.org/10.1073/pnas.2004598117

586 Meeske, A. J., Sham, L.-T., Kimsey, H., Koo, B.-M., Gross, C. A., Bernhardt, T. G., & Rudner,
587 D. Z. (2015). MurJ and a novel lipid II flippase are required for cell wall biogenesis in
588 *Bacillus subtilis*. *Proceedings of the National Academy of Sciences*, *112*(20), 6437–6442.
589 https://doi.org/10.1073/pnas.1504967112
590 Mitchell, S. L., Kearns, D. B., & Carlson, E. E. (2023). Penicillin-binding protein redundancy in
591 *Bacillus subtilis* enables growth during alkaline shock. *bioRxiv*, 2023.03.20.533529.
592 https://doi.org/10.1101/2023.03.20.533529
593 Mueller, E. A., Egan, A. J., Breukink, E., Vollmer, W., & Levin, P. A. (2019). Plasticity of
594 *Escherichia coli* cell wall metabolism promotes fitness and antibiotic resistance across
595 environmental conditions. *eLife*, *8*, e40754. https://doi.org/10.7554/eLife.40754
596 Nelson, M. E., Little, J. L., & Kristich, C. J. (2024). Pbp4 provides transpeptidase activity to the
597 FtsW-PbpB peptidoglycan synthase to drive cephalosporin resistance in *Enterococcus*
598 *faecalis. Antimicrobial Agents and Chemotherapy*, *68*(9), e00555-24.
599 https://doi.org/10.1128/aac.00555-24
600 Ng, Y. K., Ehsaan, M., Philip, S., Collery, M. M., Janoir, C., Collignon, A., Cartman, S. T., &
601 Minton, N. P. (2013). Expanding the Repertoire of Gene Tools for Precise Manipulation
602 of the *Clostridium difficile* Genome: Allelic Exchange Using pyrE Alleles. *PLOS ONE*,
603 *8*(2), e56051. https://doi.org/10.1371/journal.pone.0056051
604 Nonejuie, P., Burkart, M., Pogliano, K., & Pogliano, J. (2013). Bacterial cytological profiling
605 rapidly identifies the cellular pathways targeted by antibacterial molecules. *Proceedings*
606 *of the National Academy of Sciences*, *110*(40), 16169–16174.
607 https://doi.org/10.1073/pnas.1311066110
608 Pishdadian, K., Fimlaid, K. A., & Shen, A. (2015). SpoIIID-mediated regulation of σK function
609 during *Clostridium difficile* sporulation. *Molecular Microbiology*, *95*(2), 189–208.
610 https://doi.org/10.1111/mmi.12856
611 Pogliano, J., Osborne, N., Sharp, M. D., Abanes-De Mello, A., Perez, A., Sun, Y.-L., & Pogliano,
612 K. (1999). A vital stain for studying membrane dynamics in bacteria: A novel mechanism
613 controlling septation during *Bacillus subtilis* sporulation. *Molecular Microbiology*, *31*(4),
614 1149–1159. https://doi.org/10.1046/j.1365-2958.1999.01255.x

615 Rohs, P. D. A., & Bernhardt, T. G. (2021). Growth and Division of the Peptidoglycan Matrix.
616 *Annual Review of Microbiology*, *75*(1), 315–336. https://doi.org/10.1146/annurev-micro-
617 020518-120056
618 Sassine, J., Xu, M., Sidiq, K. R., Emmins, R., Errington, J., & Daniel, R. A. (2017). Functional
619 redundancy of division specific penicillin-binding proteins in *Bacillus subtilis*. *Molecular*
620 *Microbiology*, *106*(2), 304–318. https://doi.org/10.1111/mmi.13765
621 Saujet, L., Pereira, F. C., Serrano, M., Soutourina, O., Monot, M., Shelyakin, P. V., Gelfand, M.
622 S., Dupuy, B., Henriques, A. O., & Martin-Verstraete, I. (2013). Genome-wide analysis of
623 cell type-specific gene transcription during spore formation in *Clostridium difficile*. *PLoS*
624 *Genetics*, *9*(10), e1003756. https://doi.org/10.1371/journal.pgen.1003756
625 Sauvage, E., Kerff, F., Terrak, M., Ayala, J. A., & Charlier, P. (2008). The penicillin-binding
626 proteins: Structure and role in peptidoglycan biosynthesis. *FEMS Microbiology Reviews*,
627 *32*(2), 234–258. https://doi.org/10.1111/j.1574-6976.2008.00105.x
628 Schindelin, J., Arganda-Carreras, I., Frise, E., Kaynig, V., Longair, M., Pietzsch, T., Preibisch, S.,
629 Rueden, C., Saalfeld, S., Schmid, B., Tinevez, J.-Y., White, D. J., Hartenstein, V., Eliceiri,
630 K., Tomancak, P., & Cardona, A. (2012). Fiji: An open-source platform for biological-
631 image analysis. *Nature Methods*, *9*(7), Article 7. https://doi.org/10.1038/nmeth.2019
632 Shlosman, I., Fivenson, E. M., Gilman, M. S. A., Sisley, T. A., Walker, S., Bernhardt, T. G.,
633 Kruse, A. C., & Loparo, J. J. (2023). Allosteric activation of cell wall synthesis during
634 bacterial growth. *Nature Communications*, *14*(1), Article 1.
635 https://doi.org/10.1038/s41467-023-39037-9
636 Shrestha, S., Taib, N., Gribaldo, S., & Shen, A. (2023). Diversification of division mechanisms in
637 endospore-forming bacteria revealed by analyses of peptidoglycan synthesis in
638 *Clostridioides difficile*. *Nature Communications*, *14*(1), 7975.
639 https://doi.org/10.1038/s41467-023-43595-3
640 Sjodt, M., Rohs, P. D. A., Gilman, M. S. A., Erlandson, S. C., Zheng, S., Green, A. G., Brock, K.
641 P., Taguchi, A., Kahne, D., Walker, S., Marks, D. S., Rudner, D. Z., Bernhardt, T. G., &
642 Kruse, A. C. (2020). Structural coordination of polymerization and crosslinking by a
643 SEDS–bPBP peptidoglycan synthase complex. *Nature Microbiology*, *5*(6), Article 6.
644 https://doi.org/10.1038/s41564-020-0687-z

645 Srikhanta, Y. N., Hutton, M. L., Awad, M. M., Drinkwater, N., Singleton, J., Day, S. L.,
646 Cunningham, B. A., McGowan, S., & Lyras, D. (2019). Cephamycins inhibit pathogen
647 sporulation and effectively treat recurrent *Clostridioides difficile* infection. *Nature*
648 *Microbiology*, *4*(12), 2237–2245. https://doi.org/10.1038/s41564-019-0519-1
649 Taguchi, A., Welsh, M. A., Marmont, L. S., Lee, W., Sjodt, M., Kruse, A. C., Kahne, D.,
650 Bernhardt, T. G., & Walker, S. (2019). FtsW is a peptidoglycan polymerase that is
651 functional only in complex with its cognate penicillin-binding protein. *Nature*
652 *Microbiology*, *4*(4), Article 4. https://doi.org/10.1038/s41564-018-0345-x
653 Tan, I. S., & Ramamurthi, K. S. (2014). Spore formation in *Bacillus subtilis*. *Environmental*
654 *Microbiology Reports*, *6*(3), 212–225. https://doi.org/10.1111/1758-2229.12130
655 Tsang, M.-J., & Bernhardt, T. G. (2015). A role for the FtsQLB complex in cytokinetic ring
656 activation revealed by an *ftsL* allele that accelerates division. *Molecular Microbiology*,
657 *95*(6), 925–944. https://doi.org/10.1111/mmi.12905
658 Wielders, C. L. C., Fluit, A. C., Brisse, S., Verhoef, J., & Schmitz, F. J. (2002). *mecA* Gene Is
659 Widely Disseminated in *Staphylococcus aureus* Population. *Journal of Clinical*
660 *Microbiology*, *40*(11), 3970–3975. https://doi.org/10.1128/JCM.40.11.3970-3975.2002
661 Yanouri, A., Daniel, R. A., Errington, J., & Buchanan, C. E. (1993). Cloning and sequencing of
662 the cell division gene *pbpB*, which encodes penicillin-binding protein 2B in *Bacillus*
663 *subtilis*. *Journal of Bacteriology*, *175*(23), 7604–7616.
664 https://doi.org/10.1128/jb.175.23.7604-7616.1993
665 Zapun, A., Contreras-Martel, C., & Vernet, T. (2008). Penicillin-binding proteins and β-lactam
666 resistance. *FEMS Microbiology Reviews*, *32*(2), 361–385. https://doi.org/10.1111/j.1574-
667 6976.2007.00095.x
668
669
670